DC Electric Springs – An Emerging Technology for DC Grids

Kwan-Tat Mok*, Ming-Hao Wang*, Siew-Chong Tan*†
*Department of Electrical and Electronic Engineering
The University of Hong Kong, Hong Kong
†Email: sctan@eee.hku.hk

Shu-Yuen (Ron) Hui*‡
‡Department of Electrical and Electronic Engineering
Imperial College London, U.K.

***Abstract*—There is widespread attention on integrating renewable energy sources, such as the solar power, to DC distributed power systems and DC microgrids. The voltage stability and the power quality issues are of concern if a large proportion of power sources in these DC power systems are generated by intermittent renewable energy sources. This paper presents an electric active suspension technology known as the DC electric springs for stabilizing and improving the quality of the power distributions in DC power grids. The basic operating modes and characteristic of a DC electric spring under different types of serially-connected non-critical loads will first be introduced. Then, various potential issues that affect the power quality of the DC power systems, namely the bus voltage instability, voltage droop, system fault, and harmonics, are briefly addressed. Laboratory-scale experiments validated that the aforementioned quality issues can be mitigated using the proposed DC electric spring technology.**

***Keywords*—Smart load, distributed power systems, power electronics, electric springs, DC grids, smart grid.**

I. Introduction

There is a growing interest in using direct current (DC) power systems and DC microgrids for our electricity distribution, especially for small-scale commercial and residential applications [1], [2]. Different voltage levels on DC power distribution systems have been proposed, such as that of 48 V, 120 V, 230 V, 325 V, and 400 V [3]–[6]. There is an increasing number of renewable distributed generations, such as small-scale photovoltaic systems, being connected to DC power networks [5]. The injection of intermittent renewable energy sources into these power systems without proper control and management can cause stability problems [7].

The AC electric spring (ES) technology is a type of the demand side management solution, which was initially used to stabilize the AC power grid voltage. So far, three versions of ES have been developed. The first two versions involve the use of an ES connected in series with a non-critical load (such as thermal heaters) [8]–[11]. Consequently, the ES and the non-critical load form a smart load that can adaptively consume active and reactive power according to the availability of intermittent power generation. The third version of ES can be incorporated into an existing bidirectional AC-DC grid connected inverter commonly used for solar and wind power systems without association with any non-critical load [12]. So far, different functionalities of the ES have been explored. In [10], the possibility of ES in providing both active and reactive power compensation is addressed. This enables ES to provide additional functions of power factor correction, energy storage, and power control of non-critical loads, on top of its core function of grid voltage stabilization. In [11], it is illustrated that ES can be used to reduce the energy storage capacity of future power grid systems. Up to now, all reports on ES are related to AC power system applications [8]–[11]. There is currently no report on the application of ES on DC power systems.

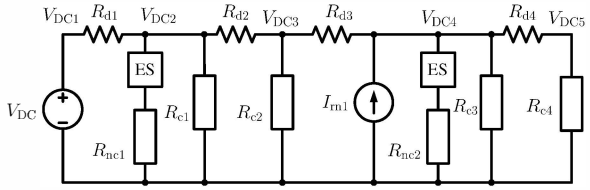

Fig. 1. Radial DC network with DC-ES installed.

This paper proposes the concept of DC electric springs (DC-ES) for applications in DC power grids. This is possibly the first attempt on using an ES to assist in the regulation of the voltage level of the busbar of a DC microgrid, and possibly the DC transmission lines. Here, the DC-ES are serially-connected to a non-critical load, thereby forming a smart load.

Similar to AC mains with a specified voltage tolerance, it is anticipated that new specifications and regulations on governing voltage tolerances of DC power grids will be established. Hence, a proper regulation of DC bus voltages is required in the future DC power systems. Therefore, the DC-ES can possibly be used for (i) regulating the DC bus voltage within the required limits while enduring the fluctuations of intermittent energy sources or deep voltage sags of power faults and (ii) performing load boosting and shedding functions to match the power consumption of the DC loads to the renewable power generation connected to the DC grids. An example of a radial DC network is shown in Fig. 1. Here, $V_{\rm DC}$ is the supply side voltage, $R_{\rm c1}$ to $R_{\rm c4}$ are the critical loads, and $R_{\rm nc1}$ and $R_{\rm nc2}$ are the non-critical loads connected to the network. The intermittent renewable energy source is represented by $I_{\rm rn1}$. It should be noted that the distributed line impedances ($R_{\rm d1}$ to $R_{\rm d4}$) between any two points on the DC network must be considered.

II. Operating Principle of DC Electric Springs

This section provides an analysis on the characteristics of the DC-ES in different regions of operation. The basic

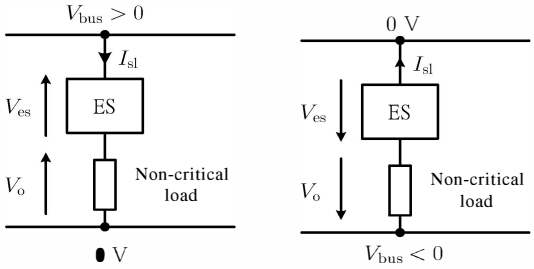

(a) DC-ES installed on positive DC bus.

(b) DC-ES installed on negative DC bus.

Fig. 2. DC-ES connected to a non-critical load in series.

configurations of series-connected DC-ES installed on positive and negative DC buses are shown in Fig. 2(a) and Fig. 2(b), respectively. The polarity definitions of the ES voltage and non-critical voltage are shown in the figures. The positive direction of the smart load current (i.e., the ES current and non-critical load current) is directed towards the ground (0 V). Here, it is assumed that the DC bus voltage $V_{\rm bus}$ is constant and equal to a nominal reference value $V_{\rm bus\_Ref}$. Hence, the impedance of the distribution lines is not taken into consideration in this section.

Generally, non-critical DC loads can be classified into four types, and they are

1. Positive constant-resistive loads;
2. Negative constant-resistive loads;
3. Positive constant-power loads;
4. Negative constant-power loads.

The terminology "positive loads" implies they are power sinks and electrical power is consumed by the load. All loads consuming energy are in this category. Conversely, "negative loads" implies power sources and electric power is delivered by the negative load. The characteristic and operating regions of these smart loads will be discussed.

A. Constant-Resistive Non-Critical Loads Connected to DC-ES

With constant-resistive loads, there are four possible configurations, namely, (i) positive load on a positive DC bus, (ii) positive load on a negative DC bus, (iii) negative load on a positive DC bus, and (iv) negative load on a negative bus. Consider that the non-critical load shown in Fig. 2(a) and Fig. 2(b) is a constant-resistive load with a value $R_{\rm o}$. The relationship between the smart load current $I_{\rm sl}$, the ES voltage $V_{\rm es}$, and the DC bus voltage $V_{\rm bus}$ is

$$\begin{aligned} V_{\rm bus} &= V_{\rm es} + V_{\rm o} \\ &= V_{\rm es} + I_{\rm sl} R_{\rm o} \end{aligned} \tag{1}$$

Using (1), the ES power $P_{\rm es}$, the non-critical load power $P_{\rm o}$, and the smart load power $P_{\rm sl}$ (summation of the ES power and the non-critical load power) can be expressed as

$$P_{\rm es} = V_{\rm es} I_{\rm sl} = \frac{V_{es}(V_{bus} - V_{\rm es})}{R_{\rm o}} \tag{2}$$

$$P_{\rm o} = V_{\rm o} I_{\rm sl} = \frac{(V_{\rm bus} - V_{\rm es})^2}{R_{\rm o}} \tag{3}$$

and

$$P_{\rm sl} = V_{\rm bus} I_{\rm sl} = \frac{V_{\rm bus}(V_{\rm bus} - V_{\rm es})}{R_{\rm o}} \tag{4}$$

From (4), it is observed that the smart load power $P_{\rm sl}$ decreases linearly with the ES voltage for constant-positive-resistive load and increases linearly with the ES voltage for constant-negative-resistive load.

Equations (1) to (4) are valid for both positive or negative DC bus voltage with either positive or negative value of constant-resistive non-critical loads. Considering the example where the DC bus voltage is positive and the non-critical load is positive constant-resistive, we have

$$I_{\rm sl} \begin{cases} > I_{\rm nsl} & \text{for } V_{\rm es} < 0 \\ < I_{\rm nsl} & \text{for } V_{\rm es} > 0 \end{cases} \tag{5}$$

$$P_{\rm es} \begin{cases} > 0 & \text{for } 0 < V_{\rm es} < V_{\rm bus\_Ref} \\ < 0 & \text{for } V_{\rm es} < 0 \text{ or } V_{\rm es} > V_{\rm bus\_Ref} \end{cases} \tag{6}$$

$$P_{\rm o} \begin{cases} > P_{\rm nsl} & \text{for } V_{\rm es} < 0 \text{ or } V_{\rm es} > 2V_{\rm bus\_Ref} \\ < P_{\rm nsl} & \text{for } 0 < V_{\rm es} < 2V_{\rm bus\_Ref} \end{cases} \tag{7}$$

and

$$P_{\rm sl} \begin{cases} > P_{\rm nsl} & \text{for } V_{\rm es} < 0 \\ < P_{\rm nsl} & \text{for } V_{\rm es} > 0 \end{cases} \tag{8}$$

where $I_{\rm nsl}$ and $P_{\rm nsl}$ are respectively the nominal smart load current and nominal smart load power, which are respectively calculated using (1) and (4) with ES being turned off, i.e., $V_{\rm es} = 0$ V.

Figure 3 shows the smart load current, the ES power, the non-critical load power, and the smart load power versus the ES voltage where the base voltage, the base current and the base power for the per unit conversion are $V_{\rm bus}$, $I_{\rm nsl}$ and $P_{\rm nsl}$, respectively. The graph is divided into four regions indicating there are four modes of operation (Fig. 3). Table I summarizes the conditions of the system in these four regions.

TABLE I. MODES OF OPERATION OF DC-ES ON POSITIVE DC BUS WITH A POSITIVE CONSTANT-RESISTIVE NON-CRITICAL LOAD

Region	$V_{\rm es}$ **range**	$I_{\rm sl}$	$P_{\rm es}$	$P_{\rm o}$	$P_{\rm sl}$
1	$V_{\rm es} < 0$	$> I_{\rm nsl}$	< 0	$> P_{\rm nsl}$	$> P_{\rm nsl}$
2	$0 < V_{\rm es} < V_{\rm bus}$	$< I_{\rm nsl}$	> 0	$< P_{\rm nsl}$	$< P_{\rm nsl}$
3	$V_{\rm bus\_Ref} < V_{\rm es} < 2V_{\rm bus\_Ref}$	$< I_{\rm nsl}$	< 0	$< P_{\rm nsl}$	$< P_{\rm nsl}$
4	$2V_{\rm bus} < V_{\rm es}$	$< I_{\rm nsl}$	< 0	$> P_{\rm nsl}$	$< P_{\rm nsl}$

B. Constant-Power Non-critical Loads Connected to DC-ES

Similarly, there are four possible configurations of a smart load implemented by a DC-ES with a serially-connected constant-power non-critical load. Considering the non-critical loads shown in Fig. 2(a) and Fig. 2(b) are constant-power loads with a value $P_{\rm o}$. The relationship between the smart load current, the ES voltage and the DC bus voltage is

$$\begin{aligned} V_{\rm bus} &= V_{\rm es} + V_{\rm o} \\ &= V_{\rm es} + \frac{P_{\rm o}}{I_{\rm sl}} \end{aligned} \tag{9}$$

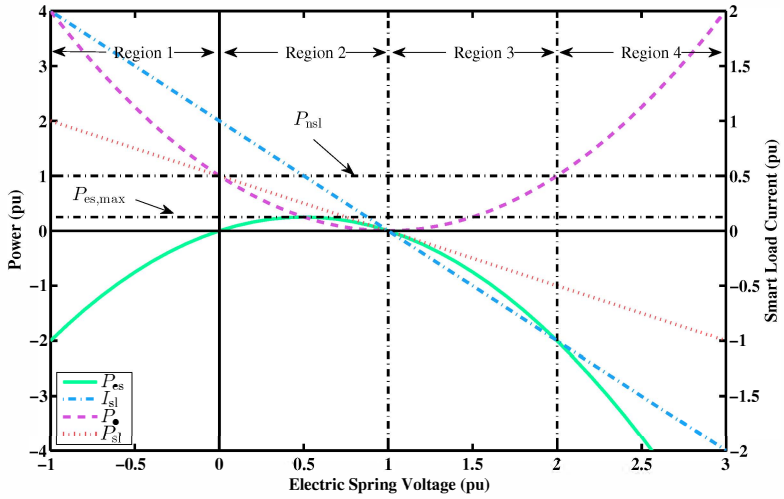

Fig. 3. The characteristic of a smart load implemented by a DC-ES with a constant-resistive non-critical load connected in series.

Using (9), the ES power and the smart load power can be expressed as

$$P_{\rm es} = \frac{V_{\rm es}P_{\rm o}}{(V_{\rm bus} - V_{\rm es})} \tag{10}$$

and

$$P_{\rm sl} = \frac{V_{\rm bus}P_{\rm o}}{(V_{\rm bus} - V_{\rm es})} \tag{11}$$

Equations (9) to (11) are valid for both positive or negative DC bus voltage with either positive or negative value of constant-power non-critical loads. Considering the case where the DC bus voltage is positive and the non-critical load is a positive constant-power load, we have

$$I_{\rm sl}\begin{cases} > I_{\rm nsl} & \text{for } 0 < V_{\rm es} < V_{\rm bus\_Ref} \\ < I_{\rm nsl} & \text{for } V_{\rm es} > 0 \text{ or } V_{\rm es} > V_{\rm bus\_Ref} \end{cases} \tag{12}$$

$$P_{\rm es}\begin{cases} > 0 & \text{for } 0 < V_{\rm es} < V_{\rm bus\_Ref} \\ < 0 & \text{for } V_{\rm es} > 0 \text{ or } V_{\rm es} > V_{\rm bus\_Ref} \end{cases} \tag{13}$$

and

$$P_{\rm sl}\begin{cases} > P_{\rm nsl} & \text{for } 0 < V_{\rm es} < V_{\rm bus\_Ref} \\ < P_{\rm nsl} & \text{for } V_{\rm es} > 0 \text{ or } V_{\rm es} > V_{\rm bus\_Ref} \end{cases} \tag{14}$$

Figure 4 shows the smart load current, the ES power, the non-critical load power and the smart load power versus the ES voltage where the base voltage, the base power and the base current for the per unit conversion are $V_{\rm bus\_Ref}$, $P_{\rm o}$ and $I_{\rm nsl}$, respectively. $I_{\rm nsl}$ is the nominal smart load current calculated using (9) when $V_{\rm es} = 0$ V. The graph is divided into three regions indicating there are three modes of operation. Table II summarizes the conditions of the system in these three regions.

III. Issues on DC Power Systems

In the previous analysis, it was assumed that the DC bus voltage is constant. In a realistic DC power system, the DC bus voltage is disturbed and the DC-ES will be used to regulate the DC bus voltage within the permitted limits. This section is focused on identifying the possible issues related to DC bus voltage disturbance. The DC power system shown in Fig. 1 is a simplified model of a realistic DC power system. There are several non-ideal factors that exist on such systems. First, parasitic resistances exist on the power distribution lines. Second, the DC source $V_{\rm DC}$ is a finite power source. Third, loads on the DC bus can inject harmonic disturbance into the bus. Fourth, the occurrences of equipment or system faults are unavoidable. By considering these factors, different types of disturbances on the DC bus voltage are possible and will be discussed. The role of DC-ES is to alleviate the effects of these disturbances which may affect the voltage stability of the DC bus.

TABLE II. Modes of Operation of DC-ES on Positive DC Bus with a Positive Constant-Power Non-Critical Load

Region	$V_{\rm es}$ range	$I_{\rm sl}$	$P_{\rm es}$	$P_{\rm sl}$
1	$V_{\rm es} < 0$	$< I_{\rm nsl}$	< 0	$< P_{\rm nsl}$
2	$0 < V_{\rm es} < V_{\rm bus}$	$> I_{\rm nsl}$	> 0	$> P_{\rm nsl}$
3	$V_{\rm bus} < V_{\rm es}$	$< I_{\rm nsl}$	< 0	$< P_{\rm nsl}$

1) Unstable DC Bus Voltage: In typical DC power systems, the DC bus is not always maintained at a stable level. The DC bus voltage level varies with time as shown in Fig. 5(a). The causes of the variation include (i) supply side voltage being unstable, (ii) intermittency of renewable energy sources, and (iii) load power variation. The time-scale of the variation can vary widely.

2) Droop Effect: Due to the presence of distribution line impedance, there is voltage drop along the distribution network. Hence, the voltage level at each point of the DC bus is different. The droop effect will increasingly reduce the voltage level as the distribution line point moves further away from the power source. Moreover, the voltage drop varies with the loading condition. As shown in Fig. 5(b), a heavy load condition can cause the voltage level at certain location of the network to drop below the allowable limits of DC bus

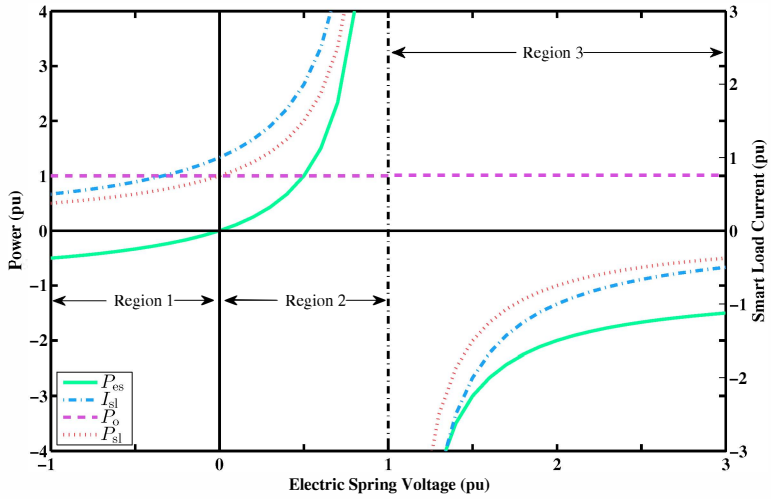

Fig. 4. An example of the characteristic of a smart load implemented by a DC-ES with a constant-power non-critical load connected in series.

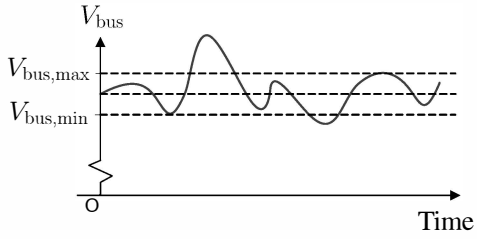

(a) An unstable DC bus voltage

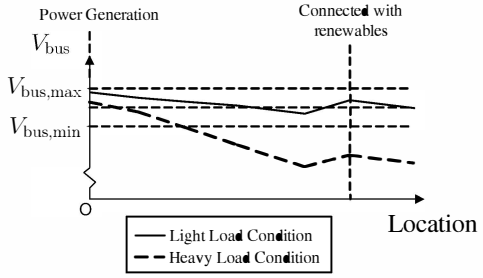

(b) Droop effect of a radial DC network due to the existence of distribution line resistance

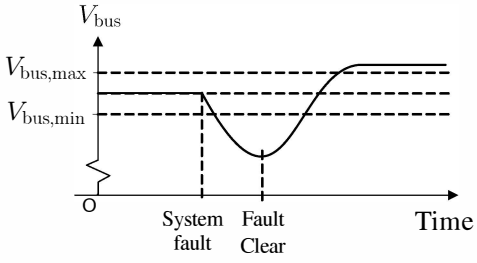

(c) A sudden DC bus voltage drop caused by equipment or system faults

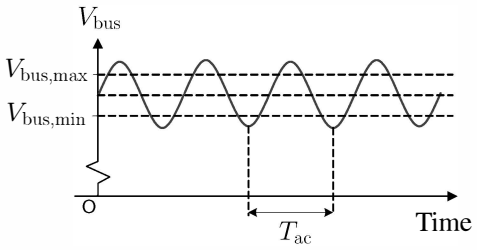

(d) DC bus voltage with substantial harmonic component

Fig. 5. Different issues on DC power systems.

voltage level, whereas there is no such issue with a light load. It is noted that, in AC power systems, the droop effect can be mitigated using distributed capacitors to provide reactive power support. However, this approach cannot be applied on DC power systems as the DC system only handles active power.

3) Equipment or System Fault: The voltage level on the DC bus can drop suddenly if there is a short circuit due to equipment or system faults, as illustrated in Fig. 5(c). When a fault occurs, there will be a sudden instantaneous voltage drop on the DC bus voltage and its voltage level may be lower than the allowable minimum level. The fault will be cleared by pre-designed protection circuits that isolates the fault location. Once returning to normal, the DC bus voltage level will be higher than the nominal value as part of the loads would have been disconnected from the DC bus.

4) Harmonic Issue: Harmonic noise can be generated by loads or power sources. For instance, an AC motor driving circuit implemented by a power inverter connected to a DC bus can inject harmonic current into the DC system with a harmonic frequency double the synchronous frequency of the motor. In addition, a power rectifier connecting to the DC power system can inject harmonic currents at twice the utility frequency. Figure 5(d) shows a DC bus voltage containing a substantial components harmonic of $1/T_{\rm ac}$. If the amplitude of harmonic content is too large, the ripple on the DC bus can exceed the voltage limits of the busbar.

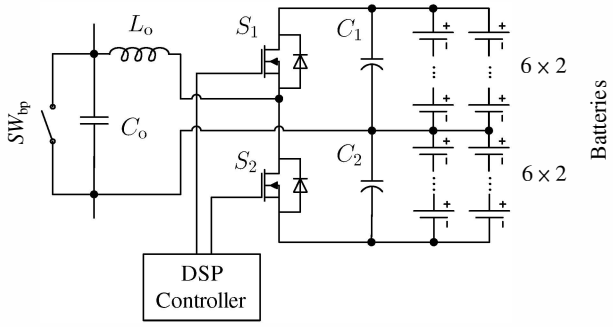

Fig. 6. The power-stage schematic of the DC-ES used in the experiment.

TABLE III. SPECIFICATIONS OF THE DC-ES

Description	Parameter	Value
MOSFET switches	S_1, S_2	IRFP31N50L
Storage capacitors	C_1, C_2	1500 μF
Filter capacitor	$C_\bullet$	6.6 μF
Filter inductor	$L_\bullet$	600 μH
Batteries		LC-R127R2NA (24 pieces)
Switching frequency	f_S	20 kHz
DSP Controller		TMS320F28069

IV. EXPERIMENTAL RESULTS

The objectives of the following experiments are to demonstrate different modes of DC-ES operation and to validate the operating limits of a DC-ES for a given system against the theoretical derivations. The DC-ES is implemented using the half-bridge inverter shown in Fig. 6 and is controlled by a low-cost commercial digital signal processing controller TMS320F28069 from Texas Instruments. The specifications of the converter of the DC-ES setup is shown in TABLE III. In practice, the permitted range of the ES voltage will be bounded by the given rated ES voltage, the rated smart load current and the allowable range of the non-critical voltage, as given by

$$\begin{cases} \mathrm{V_{es\_rated\_min}} \le \mathrm{V_{es}} \le \mathrm{V_{es\_rated\_max}} \\ \mathrm{V_{o\_rated\_min}} \le \mathrm{V}o \le \mathrm{V_{o\_rated\_max}} \\ \mathrm{I_{sl\_rated\_min}} \le I_{\mathrm{sl}} \le \mathrm{I_{sl\_rated\_max}} \end{cases} \quad (15)$$

The permitted range of the ES voltage can be found using the constraints in (15) and can be expressed as

$$\mathrm{V_{es\_min}} \le \mathrm{V_{es}} \le \mathrm{V_{es\_max}} \quad (16)$$

Once the permitted range of the ES voltage is found, the operating limits of the system can be predicted. Here it is assumed that the DC-ES is operated with a suitable control to regulate the DC bus voltage to $V_{\mathrm{bus\_Ref}}$ and the ES is within the range defined in (16). The experiment is divided into two parts. Part one demonstrates the functionality of DC-ES for regulating the DC bus voltage as discussed in Section III-1. Part two demonstrates the use of DC-ES for alleviating the droop effect as described in Section III-2.

A. Part One – Unstable Supply Voltage

This experiment verifies the use of DC-ES for regulating the DC bus voltage as discussed in Section III-1. The setup of the experiment is shown in Fig. 7. The nominal DC bus voltage is set at $V_{\mathrm{bus\_Ref}} = 48$ V. The actual DC bus voltage V_{DC} is provided by a programmable DC power source,

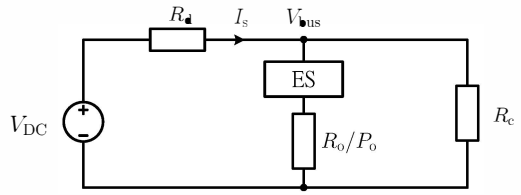

Fig. 7. An example of a DC electrical system with a DC-ES installed.

TABLE IV. SYSTEM SPECIFICATIONS OF THE EXPERIMENTAL SETUP USING CONSTANT-RESISTIVE LOAD

Description	Parameter	Value
Nominal DC bus voltage	$V_{\mathrm{bus\_Ref}}$	48 V
Distribution line resistance	R_{d}	0.37 Ω
Critical load resistance	R_{c}	14.05 Ω
Non-Critical load resistance	$R_\bullet$	15.128 Ω
Rated ES minimum voltage	$V_{\mathrm{es\_rated\_min}}$	−60 V
Rated ES maximum voltage	$V_{\mathrm{es\_rated\_max}}$	60 V
Rated smart load minimum current	$I_{\mathrm{sl\_rated\_min}}$	−12 A
Rated smart load maximum current	$I_{\mathrm{es\_rated\_max}}$	12 A
Rated non-critical load minimum voltage	$V_{\bullet\mathrm{\_rated\_min}}$	−60 V
Rated non-critical load maximum voltage	$V_{\bullet\mathrm{\_rated\_max}}$	60 V

which is programmed to give a fluctuating voltage to simulate the unstable supply side voltage source. It has the following expression:

$$V_{\mathrm{DC}} = V_{\mathrm{DC\_nom}} + \Delta V_{\mathrm{DC}} \quad (17)$$

where $V_{\mathrm{DC\_nom}}$ is the nominal supply side voltage that allows the DC bus voltage to be $V_{\mathrm{bus\_Ref}}$ without DC-ES, and ΔV_{DC} is a random fluctuating voltage. Two cases are studied in this experiment: (i) positive constant-resistive non-critical load and (ii) positive constant-power non-critical load.

1) Positive Constant-Resistive Non-Critical Load: The specifications of the experiment is shown in TABLE IV. Substituting these parameters into (15) yields

$$-24\mathrm{V} \le V_{\mathrm{es}} \le 60\mathrm{V} \quad (18)$$

which implies $V_{\mathrm{es\_min}} = -24$ V and $V_{\mathrm{es\_max}} = 60$ V. The nominal DC source voltage is found from

$$V_{\mathrm{DC\_nom}} = V_{\mathrm{bus}} \frac{(R_{\mathrm{o}} // R_{\mathrm{c}}) + R_{\mathrm{d}}}{(R_{\mathrm{o}} // R_{\mathrm{c}})} \quad (19)$$

which gives $V_{\mathrm{DC\_nom}} = 50.44$ V.

The experiment is divided into two parts. In the first part, the DC-ES is turned off and a fluctuating supply side voltage with a fluctuating profile is applied to the DC system for 300 seconds. In the second part, the DC-ES is activated and the same fluctuating profile is applied for the same time period. The experimental results are shown in Fig. 8. The measurements show that without DC-ES ($t = 0$ to 300 s), the DC bus voltage fluctuates between 45 V to 51 V. With DC-ES activated ($t = 300$ to 600 s), the DC bus voltage can be regulated, except during the short periods of T_1 and T_2. At T_1, the ES voltage reaches its minimum, $V_{\mathrm{es\_min}}$, and at T_2, it reaches its maximum, $V_{\mathrm{es\_max}}$. Therefore, the DC bus voltage cannot be regulated in these two periods of timed due to its limited capacity. Such a problem can be resolved by increasing the number of ES installed over the distributed line to support the voltage regulation.

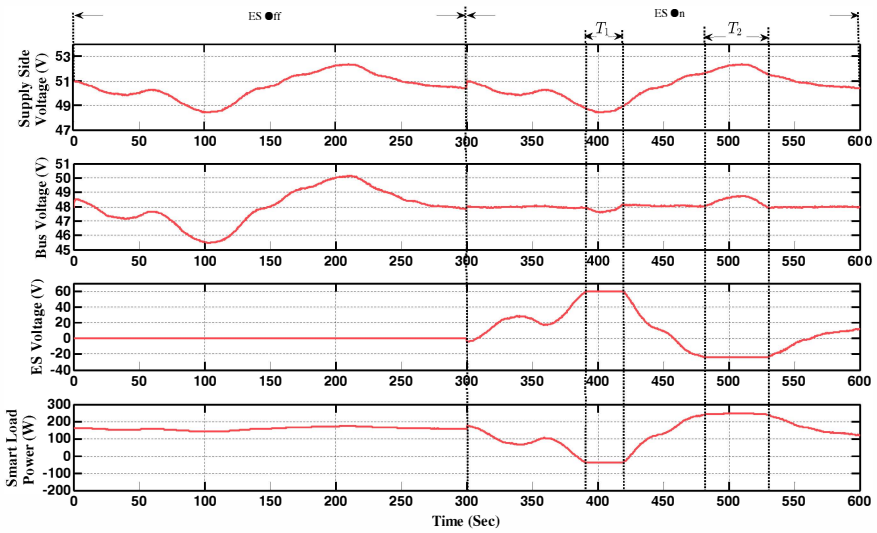

Fig. 8. Experimental result with an unstable supply side voltage variation with a constant-resistive non-critical load.

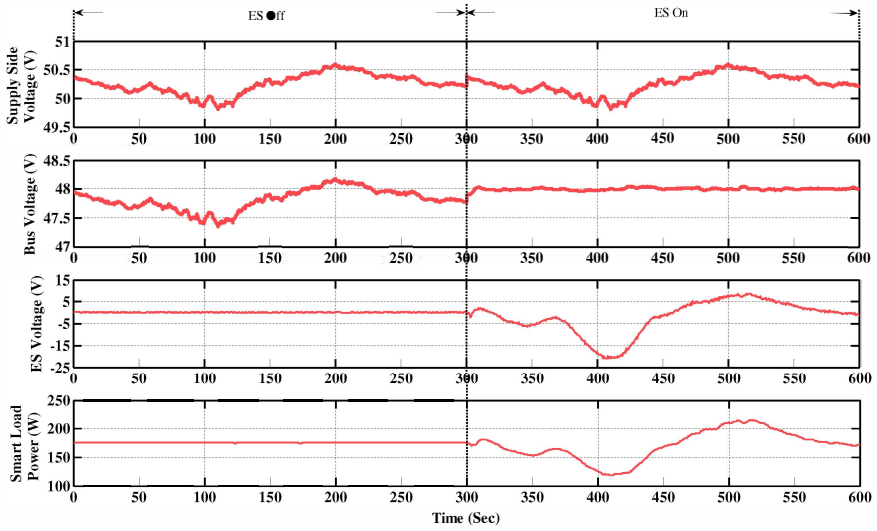

Fig. 9. Experimental result with an unstable supply side voltage variation with a constant-power non-critical load.

TABLE V. SYSTEM SPECIFICATIONS OF THE EXPERIMENTAL SETUP USING CONSTANT-POWER LOAD

Description	Parameter	Value
Nominal DC bus voltage	$V_{\text{bus\_Ref}}$	48 V
Distribution line resistance	R_{d}	0.37 Ω
Critical load resistance	R_{c}	14.05 Ω
Non-Critical load power	$P_{\bullet}$	150.78 W
Rated ES minimum voltage	$V_{\text{es\_rated\_min}}$	−60 V
Rated ES maximum voltage	$V_{\text{es\_rated\_max}}$	60 V
Rated smart load minimum current	$I_{\text{sl\_rated\_min}}$	0 A
Rated smart load maximum current	$I_{\text{es\_rated\_max}}$	12 A
Rated non-critical load minimum voltage	$V_{\bullet\text{\_rated\_min}}$	38 V
Rated non-critical load maximum voltage	$V_{\bullet\text{\_rated\_max}}$	72 V

2) Positive Constant-Power Non-Critical Load: The constant-power non-critical load is implemented using a DC–DC buck converter with its input port connected in series with the DC-ES while its output port is connected to an electronic load. The specifications of the experiment are shown in TABLE V. Substituting these parameters into (15) yields

$$-24 \text{ V} \leq V_{\text{es}} \leq 10\text{V} \tag{20}$$

which implies that $V_{\text{es\_min}} = -24$ V and $V_{\text{es\_max}} = 10$ V. The specifications of the experiment are shown in TABLE V. The nominal DC source voltage is found from

$$V_{\text{DC}} = R_{\text{d}} \left(\frac{P_{\text{o}}}{V_{\text{bus\_Ref}}} + \frac{V_{\text{bus\_Ref}}}{R_{\text{c}}} + \frac{V_{\text{bus\_Ref}}}{R_{\text{d}}} \right) \tag{21}$$

as $V_{\text{DC\_nom}} = 50.43$ V. The experiment is similar to that described in Section IV-A1. The DC-ES is turned off for the first 300 seconds and then turned on for the next 300 seconds. The experimental results are recorded in Fig. 9. It can be seen that that without DC-ES ($t = 0$ to 300 s), the DC bus voltage

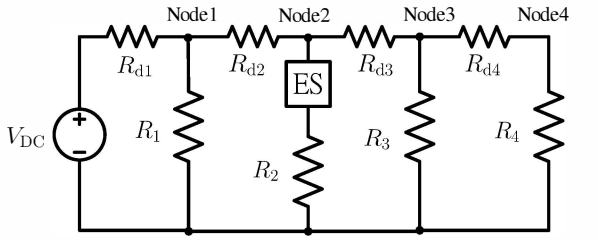

(a)

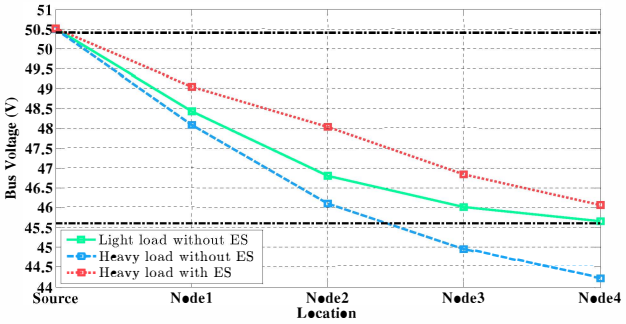

(b)

Fig. 10. (a) Experiment configuration for droop effect and (b) experimental results show the voltage level on each node.

fluctuates between 47 V to 48.5 V. With DC-ES (t = 300 to 600 s), the DC bus voltage can be regulated at all times. Since the application of negative voltage on the constant-power load (the buck converter) is prohibited, the DC-ES can only be operated in either region one ($V_{es} < 0$) or region two ($V_{es} > 0$) according to Fig. 4.

B. Part Two – Droop Effect

This experiment verifies the effectiveness of using DC-ES for alleviating the droop effect along a radial DC network. The configuration of the experiment is shown in Fig. 10(a). The parameters used in this experiment are $R_{d1} = R_{d2} = R_{d3} = R_{d4} = 0.2\ \Omega$, $R_1 = R_3 = 25\ \Omega$, $R_2 = 10\ \Omega$, and $R_4 = 25\ \Omega$ (in light load condition) or $R_4 = 12\ \Omega$ (in heavy load condition). The DC source voltage is set at $V_{DC} = 50.5$ V. The nominal DC bus voltage is $V_{bus\_Ref} = 48$ V and a 5 % allowable variation is chosen. The experiment results are given in Fig. 10.

When $R_4 = 25\ \Omega$, the DC bus voltage of all the four nodes are within the permitted voltage limits ($45.6\ \text{V} \leq V_{bus} \leq 50.4\ \text{V}$). When $R_4 = 10\ \Omega$, the DC bus voltage of node three and four exceed the minimum limit. Then, the ES is activated in such a way that the DC bus voltage of all the four nodes resume to within the voltage limits.

V. Conclusions

This is possibly the first attempt on using a power electronic device (in the form of electric springs) to assist in the regulation of the voltage level of the busbar of DC power systems. Different possible types of a non-critical load that is serially connected to the electric spring to form a smart load is analyzed. Experimental results are provided for verifying the use of DC electric springs for alleviating various power quality issues. The paper provides a fundamental understanding on the DC-ES characteristics and modes of operation, which sets a foundation for future studies on the power quality improvement and the busbar voltage regulation of DC distribution systems and DC microgrids.

Acknowledgment

This project is supported in part by the Hong Kong Research Grant Council under the Theme-based project T23-701/14-R/N.

References

[1] M. Murrill and B. J. Sonnenberg, "Evaluating the opportunity for DC power in the data center," 2010. [Online]. Available: http://www.emersonnetworkpower.com/documentation/en-us/brands/liebert/documents/white%20papers/124w-dcdata-web.pdf

[2] H. Kakigano, Y. Miura, and T. Ise, "Low-voltage bipolar-type DC microgrid for super high quality distribution," *IEEE Trans. Power Electron.*, vol. 25, no. 12, pp. 3066–3075, Dec 2010.

[3] A. Sannino, G. Postiglione, and M. H. J. Bollen, "Feasibility of a DC network for commercial facilities," *IEEE Trans. Ind. Appl.*, vol. 39, no. 5, pp. 1499–1507, Sept 2003.

[4] K. Engelen, E. Leung Shun, P. Vermeyen, I. Pardon, R. D'hulst, J. Driesen, and R. Belmans, "The feasibility of small-scale residential DC distribution systems," in *Proceedings, IEEE Industrial Electronics, IECON 2006 - 32nd Annual Conference on*, Nov 2006, pp. 2618–2623.

[5] B. Indu Rani, G. Saravana Ilango, and C. Nagamani, "Control strategy for power flow management in a PV system supplying DC loads," *IEEE Trans. Ind. Electron.*, vol. 60, no. 8, pp. 3185–3194, Aug 2013.

[6] W. Li, X. Mou, Y. Zhou, and C. Marnay, "On voltage standards for DC home microgrids energized by distributed sources," in *Proceedings, IEEE Power Electronics and Motion Control Conference (IPEMC), 2012 7th International*, vol. 3, June 2012, pp. 2282–2286.

[7] "Germany's green energy destablizing electric grids," Institute for Energy Research, Jan. 2013. [Online]. Available: http://instituteforenergyresearch.org/analysis/germanys-green-energy-destabilizing-electric-grids/

[8] S. Y. Hui, C. K. Lee, and F. F. Wu, "Electric springs - a new smart grid technology," *IEEE Trans. Smart Grid*, vol. 3, no. 3, pp. 1552–1561, 2012.

[9] S. Y. R. Hui, C. K. Lee, and F. F. Wu, "Power control circuit and method for stabilizing a power supply," Oct. 3 2011, US Patent App. 13/251,823.

[10] S. C. Tan, C. K. Lee, and S. Y. Hui, "General steady-state analysis and control principle of electric springs with active and reactive power compensations," *IEEE Trans. Power Electron.*, vol. 28, no. 8, pp. 3958–3969, 2013.

[11] C. K. Lee and S. Y. Hui, "Reduction of energy storage requirements in future smart grid using electric springs," *IEEE Trans. Smart Grid*, vol. 4, no. 3, pp. 1282–1288, Sept 2013.

[12] C. K. Lee and S. Y. R. Hui, "Input AC voltage control bi-directional power converters," May 31 2013, US Patent App. US2013/0322139.